Journal of Structural Geology, Vol. 12, No. 1, pp. 47 to 58, 1990
Printed in Great Britain

0191-8141/90 $03.00 + 0.00

Deformation around a thrust tip in Carboniferous limestone at Tutt Head, near Swansea, South Wales

A. J. HYETT

Rock Mechanics Research Group, Department of Mineral Resources Engineering, Imperial College of Science, Technology and Medicine, London SW7 2BP, U.K.

(*Received* 13 *October* 1987; *accepted in revised form* 6 *May* 1989)

Abstract—The Tutt Head thrust zone is the tip of a forward propagating lateral ramp which links two levels of detachment within the Langland–Mumbles Anticline. An early pressure-solution accommodated cataclastic phase of deformation is partially overprinted by later plastic deformation involving dislocation glide, dislocation climb and grain-boundary sliding mechanisms.

Two- and three-dimensional strain determinations indicate that displacement reduction in the tip zone is primarily accommodated by footwall extension with subsidiary contribution from hangingwall contraction. Localized oblique movement in the tip zone is explained by the process of *tip-line pinning*. Geometrical considerations reveal the requirement for diachronous emergence of the tip-line from an obstacle to propagation. This enables differential displacement about a pinning point and the consequent generation of shear strain co-planar with the thrust plane. Such shear strains are necessarily localized and limited in magnitude.

The stress pattern around the thrust tip is compatible with that predicted by the elastic solution to the stress distribution around a Mode II shear crack. The observation of a recognizable stress concentration suggests that quite high stress concentrations may accompany thrust-tip propagation.

INTRODUCTION

ELLIOTT (1976) recognized that the leading edge of a thrust fault is often marked by a zone of plastic strain, frequently incorporating folding, which he called the *ductile bead*. It is expected that compatibility problems at such locations can generate localized conditions of high stress and strain rate, with associated changes in the deformation mechanism.

The Tutt Head thrust zone (THTZ), near Swansea (Fig. 1), provides an excellent opportunity to examine the localized micro- and mesoscale deformation around a thrust tip, and in particular to apply a variety of palaeostress and strain determination techniques. The thrust tip is exposed within a coarse calcareous pellet-rich grainstone unit: pellets within which provide ideal strain markers, and the sparry calcite has pervasive *e*-twinning which was used to determine palaeostress. This paper presents field observations and microstructural data from the THTZ, and subsequently interprets some mechanical aspects of thrust fault propagation, such as the sequential development of the tip zone, dominant deformation mechanisms, strain pattern and palaeostress distribution. Although the results apply to a particular mesoscale exposure, it is probable that the important conclusions will hold for other thrust tips at much larger scales.

A limiting factor in an analysis of this kind was the requirement that sample collection minimized damage in the vicinity of the structure. Therefore, only a limited number of very small specimens were removed from the thrust tip for detailed microscopic examination. It is for this reason that the database is less extensive than would otherwise have been ideal.

FIELD SETTING AND MESOSCALE GEOMETRY

Variscan thrusting and associated folding in South Gower is associated with overthrusting and partial tectonic inversion of a late Devonian–Silesian marine shelf. The THTZ is a mesoscale structure, possibly generated to accommodate flexure of the E–W-trending Langland–Mumbles Anticline (Fig. 2). Dip orientation data collected from the anticline indicates a rounded hinge and an interlimb angle of about 65°. Shaw (1982) suggested that the interlimb angle and fold profile vary above and below the base of the Seminula Mudstone—a characteristic feature of concentric folding which frequently exhibits internal detachment and resultant disharmony. Detachment within the Langland–Mumbles Anticline probably follows the base of the Seminula Mudstone, but occasionally ramps up to its upper surface, forming minor thrust zones of limited displacement, such as the THTZ. The upper part of the Seminula Mudstone, within which the THTZ is exposed, was accurately logged (Fig. 3). The main characteristic is an anomalously thick coarse grainstone unit, within which the intense deformation associated with the thrust tip is exposed.

Layers of fibrous calcite, which ubiquitously coat the thrust plane, and smeared out clasts of brecciated vein calcite, indicate that the average movement direction was towards 018° (Fig. 4). This is approximately perpendicular to the fold hinge of the Langland–Mumbles Anticline—a result which agrees with the geometry and mechanics of flexure induced thrusting. The maximum displacement observed on the thrust was 3.5 m. The thrust plane flats dip at around 43° towards 110° and the

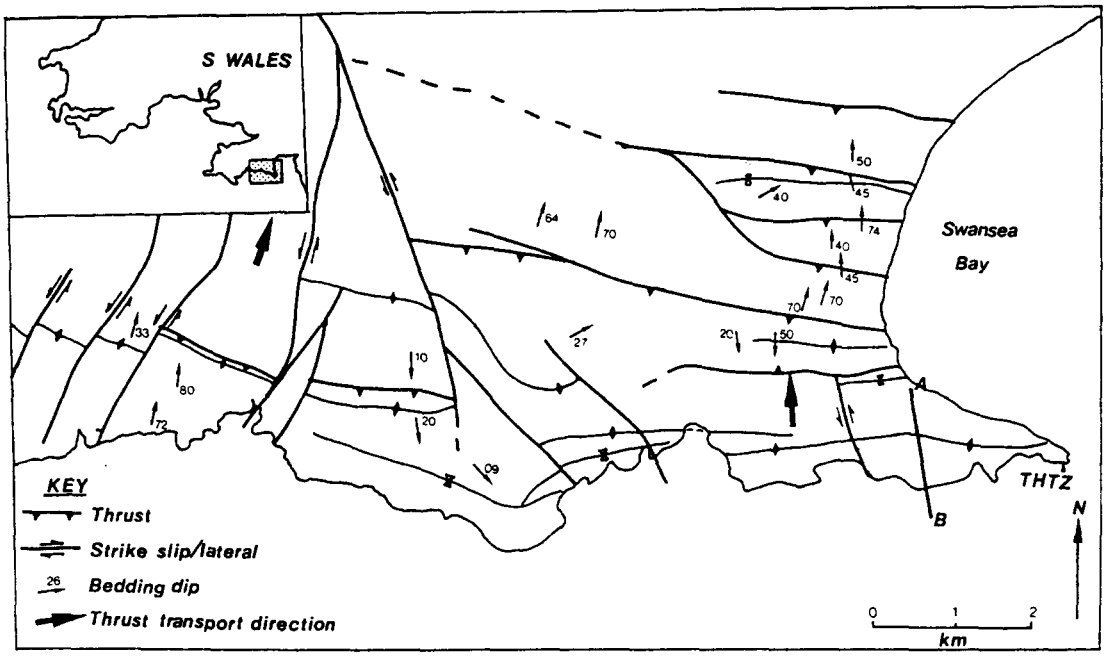

Fig. 1. Location of the Tutt Head thrust zone (THTZ).

bedding plane cut-offs trend nearly N–S, i.e. subparallel to the movement direction, which indicates an essentially lateral ramp setting for the thrust zone. The thrust tip must consequently represent the forward propagating tip of a lateral ramp (Fig. 5). Such a lateral structure may link two detachment horizons within the anticline; the lower being at the base of the Seminula Mudstone, and the upper either at the base or in the lowermost units of the Dolomitic Pseudobreccias, where inter-layer slip and local minor thrusting were observed.

A section through the tip zone, parallel to the movement direction was grid mapped in detail (Fig. 6). Attention was concentrated on the intense deformation within the coarse pellet-rich grainstone unit where displacement was observed to fall off rapidly (see below). The section in Fig. 6 was area balanced as accurately as possible, with three-dimensional strain determinations providing added constraint (Fig. 7).

DEFORMATION MECHANISMS

Deformation around the thrust tip (see Fig. 8) involved an initial phase of cataclastic deformation which was succeeded and in places overprinted by a later phase of plastic deformation. A similar transition in the predominant deformation mechanism was observed by Bowler (1987) for a thrust duplex in Cambrian quartzite near Durness, Scotland.

Cataclastic deformation

Cataclastic deformation is restricted to a narrow zone in the hangingwall of the thrust zone and a more extensive zone near the base of the grainstone unit. It records the earliest deformation within the tip zone. Initial microfracturing and veining (Fig. 9) is followed by the progressive removal of host rock along wavy pressure-

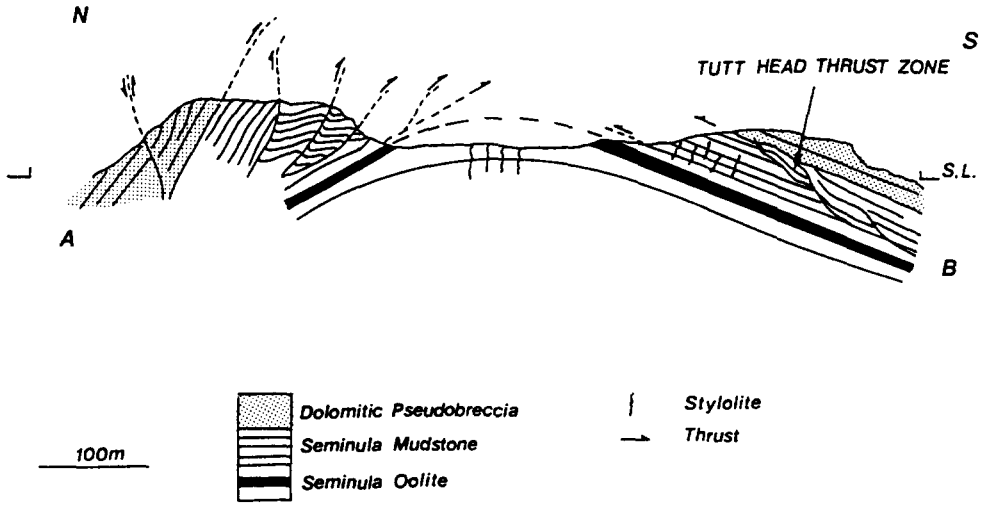

Fig. 2. N–S cross-section (A–B in Fig. 1) through the Langland–Mumbles Anticline indicating the location of the Tutt Head thrust zone (after Shaw 1982).

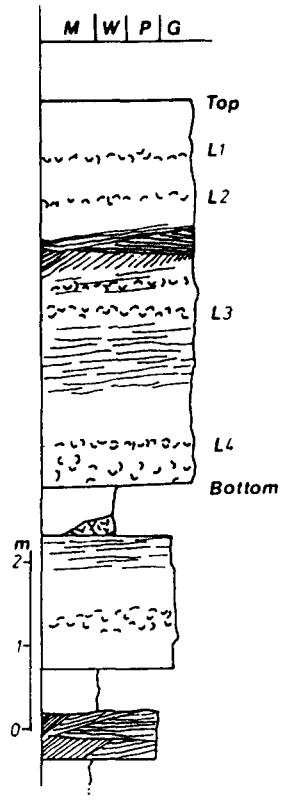

Fig. 3. Sedimentary log of the upper part of the Seminula Mudstone formation. L_1–L_4 refer to brachiopod-rich horizons (M—mudstone, W—wackestone, P—packstone, G–grainstone).

solution seams, which are lined with insoluble residues, and have been subsequently folded. The efficiency of cataclasis must be significantly reduced by the abundance of calcite in solution, which if precipitated will rapidly anneal any microcracks. Therefore pressure solution is probably necessary to accommodate cataclasis, sometimes resulting in complete removal of the host rock. It is probable that cycles of cracking and complimentary pressure solution occurred.

Plastic deformation

The progressive development of plastic microstructures within the tip zone appears to be related to the level of strain (R_s), measured by either the Fry or R_f/ϕ methods (see below).

(a) *Low strain* ($R_s < 2$)—*twinning field* (Fig. 10). Initial deformation involves *e*-twinning of the sparry calcite cement and complimentary pressure solution of pellets and mudstone clasts. The cement shows pervasive twinning indicating that the stress has been effectively distributed throughout the rock, which is an important assumption for the later palaeostress analysis. Both particles and cement deform homogeneously.

(b) *Moderate–high strain* ($2 < R_s < 5$)—*dislocation glide and climb fields* (Fig. 11). At this strain level the pellets begin to deform progressively more easily than the sparry calcite cement and brachiopod debris. This is probably related to a decrease in rigidity of the cement

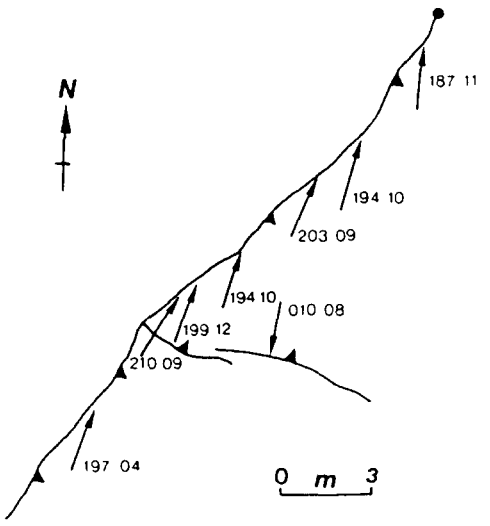

Fig 4. Movement direction data. The numbers refer to the plunge and direction of calcite fibres, and the arrowheads indicate the sense of movement. The average movement direction is towards 018°.

caused by the extensive onset of dislocation glide mechanisms, as indicated by widespread undulose extinction and kinking within large calcite crystals.

Above $R_s = 2.5$, dynamic recrystallization is observed, prospective sites being grain boundaries, twin intersections and kink bands. Shaw (1982) observed that the optical subgrain size and recrystallized grain size were similar and proposed the mechanism of subgrain rotation to explain the dynamic recrystallization.

(c) *Very high strain* ($R_s > 5$)—*grain-boundary sliding field* (Fig. 12). In the centre of the tip zone ultramylonite is generated possessing a diagnostic ribbon texture, with an average grain size of 4 μm. Shaw (1982) used electron microscopy to observe a tabular or pseudo-hexagonal grain morphology.

STRAIN ANALYSIS

This section reports the results of two- and three-dimensional strain determinations, which were performed on deformed pellets within specimens taken from around the tip of the THTZ, using the Fry and R_f/ϕ methods.

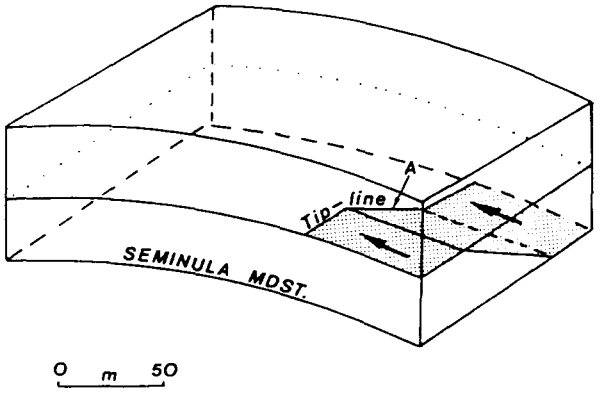

Fig. 5. Geometrical relation of the thrust zone to the detachment horizons within the Langland–Mumbles Anticline. The arrow indicates the thrust propagation direction.

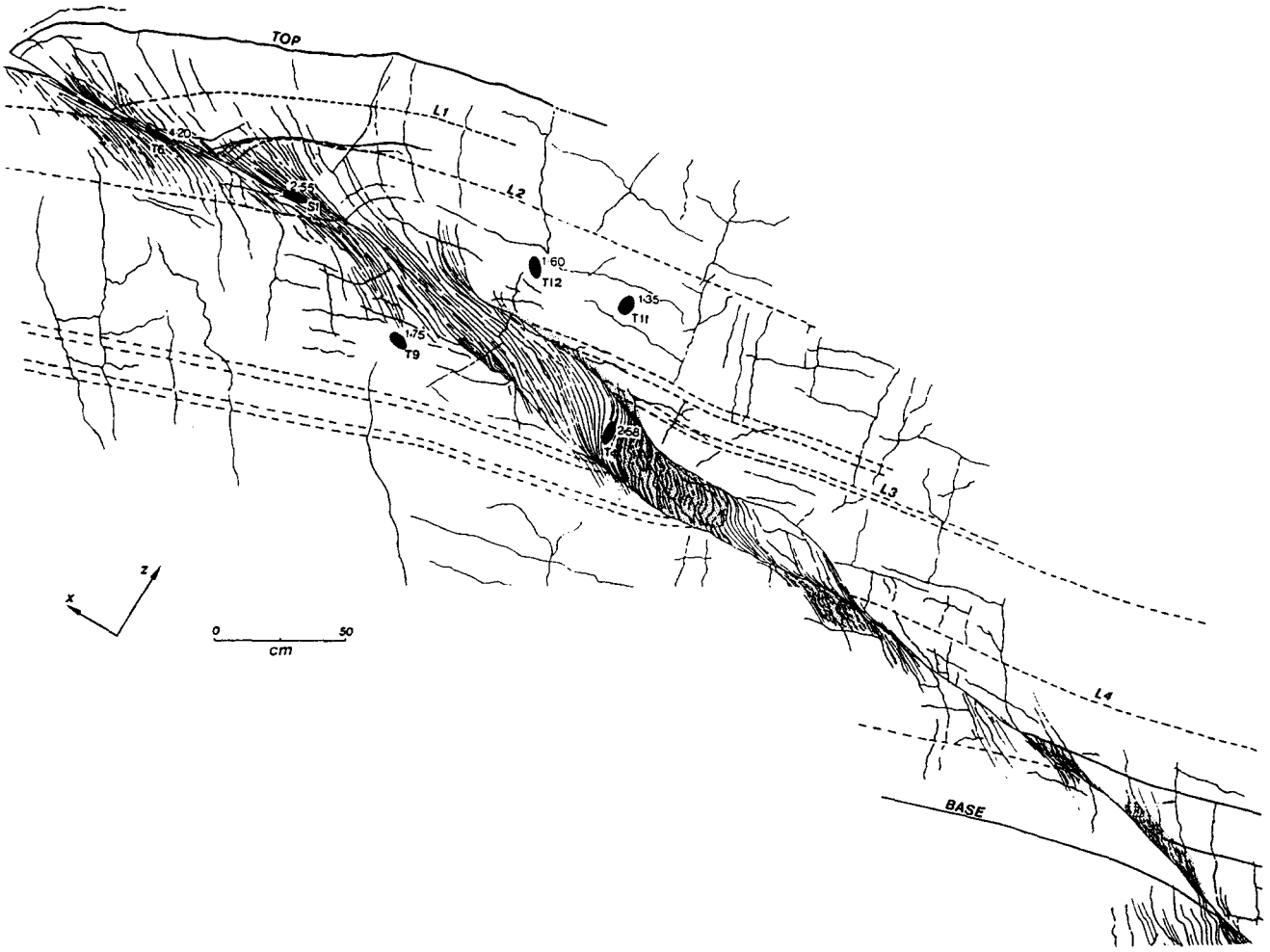

Fig. 6. Grid (30 × 30 cm) mapped section of the thrust tip sub-parallel to movement. The ellipses represent the strain ellipses in the plane of section (referred to throughout as the x–z plane, ~012°/vertical). The number refers to the strain ratio in the plane of section (e_{xz}) for each specimen (T9, S1, etc.).

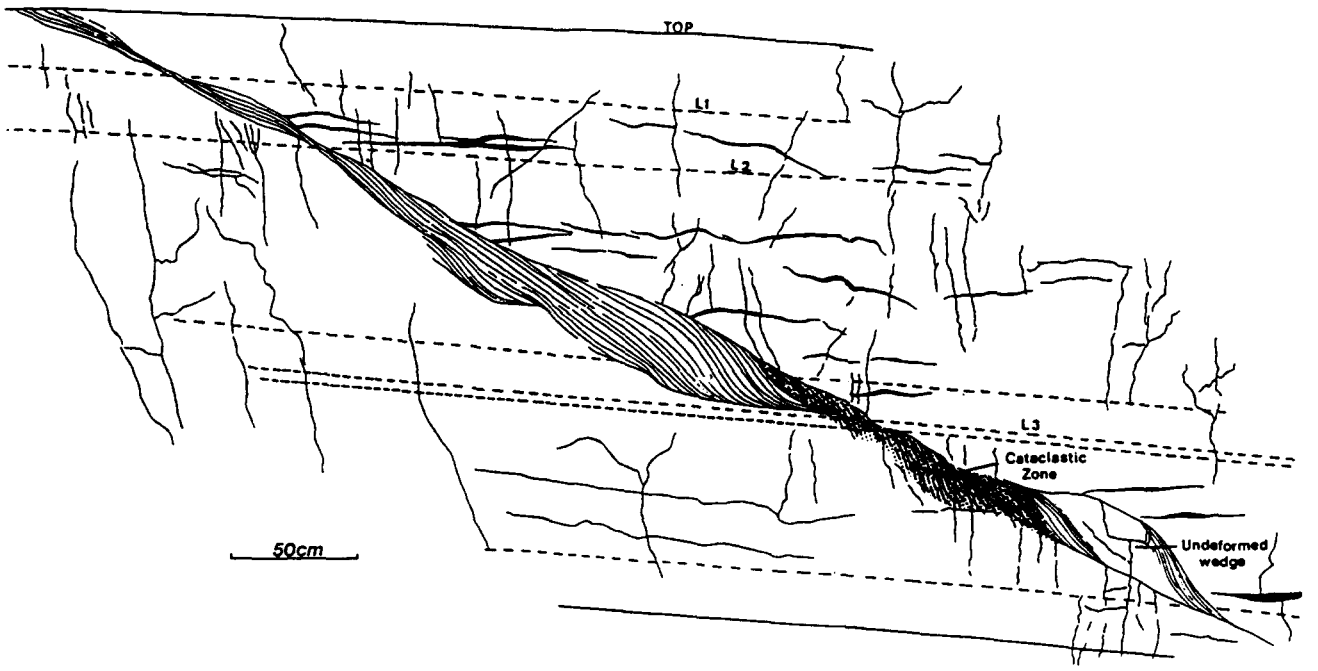

Fig. 7. Restored section constrained using accurately recorded thicknesses around the thrust tip, three-dimensional strain data and sheared, pre-thrusting, styolites.

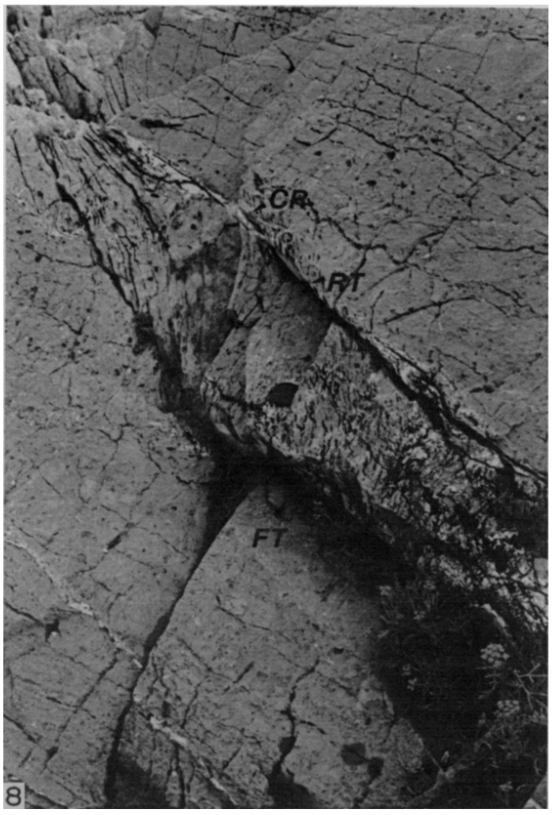

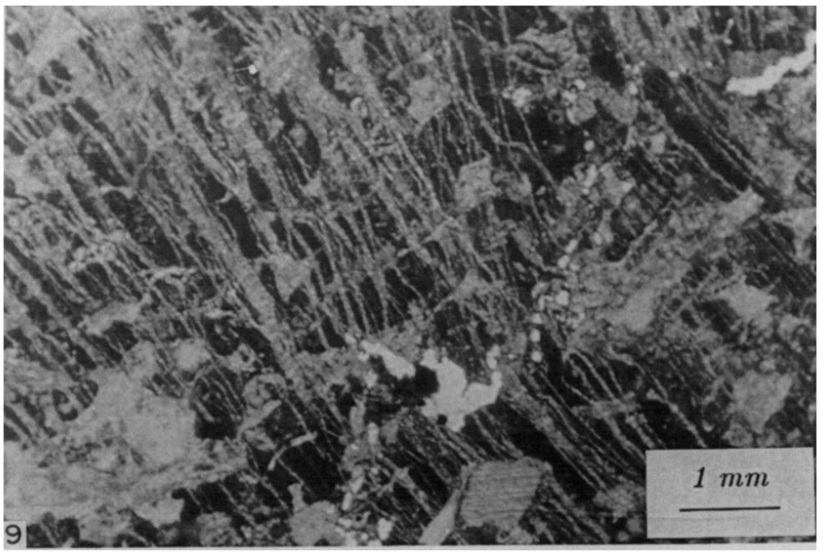

Fig. 8. Deformation at the base of the coarse grainstone unit. CR–cataclastic ribbon, CV–recrystallized vein calcite RT–roof thrust, FT–floor thrust.

Fig. 9. Initial stage microcracking in thin section.

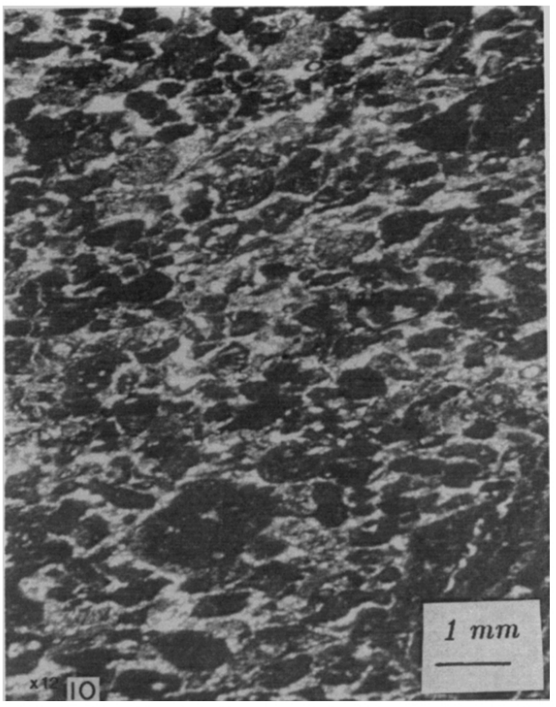

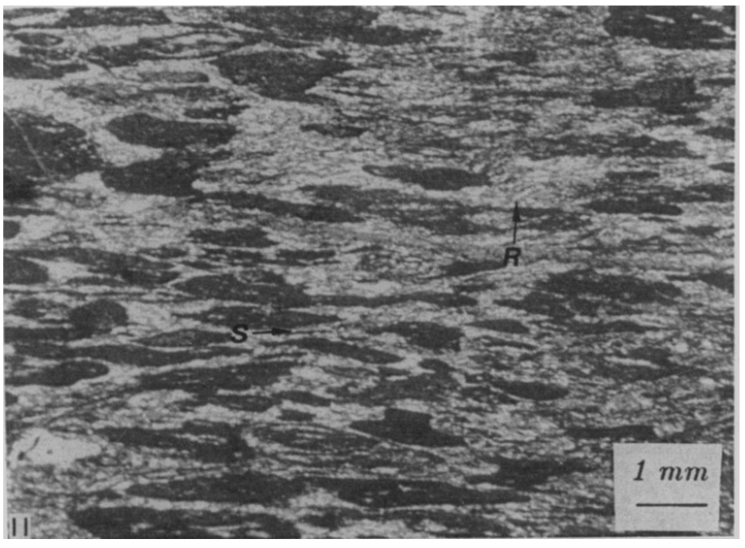

Fig. 10. Typical low strain deformation. The dark markers are pellets.

Fig. 11. Moderate to high strain deformation. Note shear bands (S), Relict twins (R). Strain ratio is approximately 2.6.

Fig. 12. Ultra-mylonite. Note characteristic ribbon texture and intact Texturlurid foram (T).

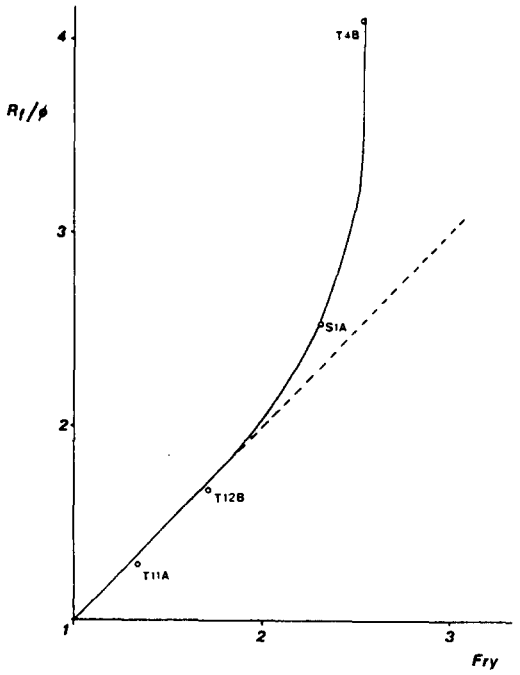

Fig. 13. The relation between strain ratios obtained from the R_f/ϕ and Fry methods.

The Fry method (Fry 1979) was extensively employed because it is fast, especially when computerized in association with a digitizing tablet. The technique exploits the redistribution of an original anti-clustered distribution of points, which occurs during deformation.

The R_f/ϕ technique was employed usually at low strain levels, when variability in marker size and initial shape imperfections make the Fry method more difficult to interpret. The R_f/ϕ estimation of bulk strain deteriorates at higher strain levels because the inherent competence contrast between the markers and the cement becomes increasingly active.

A comparison of results obtained using both techniques on the same specimens (Fig. 13), shows a divergence above $R_s \sim 2$. The Fry method was considered to estimate the bulk strain whereas the R_f/ϕ method more correctly indicated the marker strain. Evidence from various thin sections suggests that the divergence begins at the onset of pervasive plastic deformation (as opposed to *e*-twinning) of the cement. Below this threshold, although the cement deforms by *e*-twinning it remains essentially rigid, providing a framework which prevents

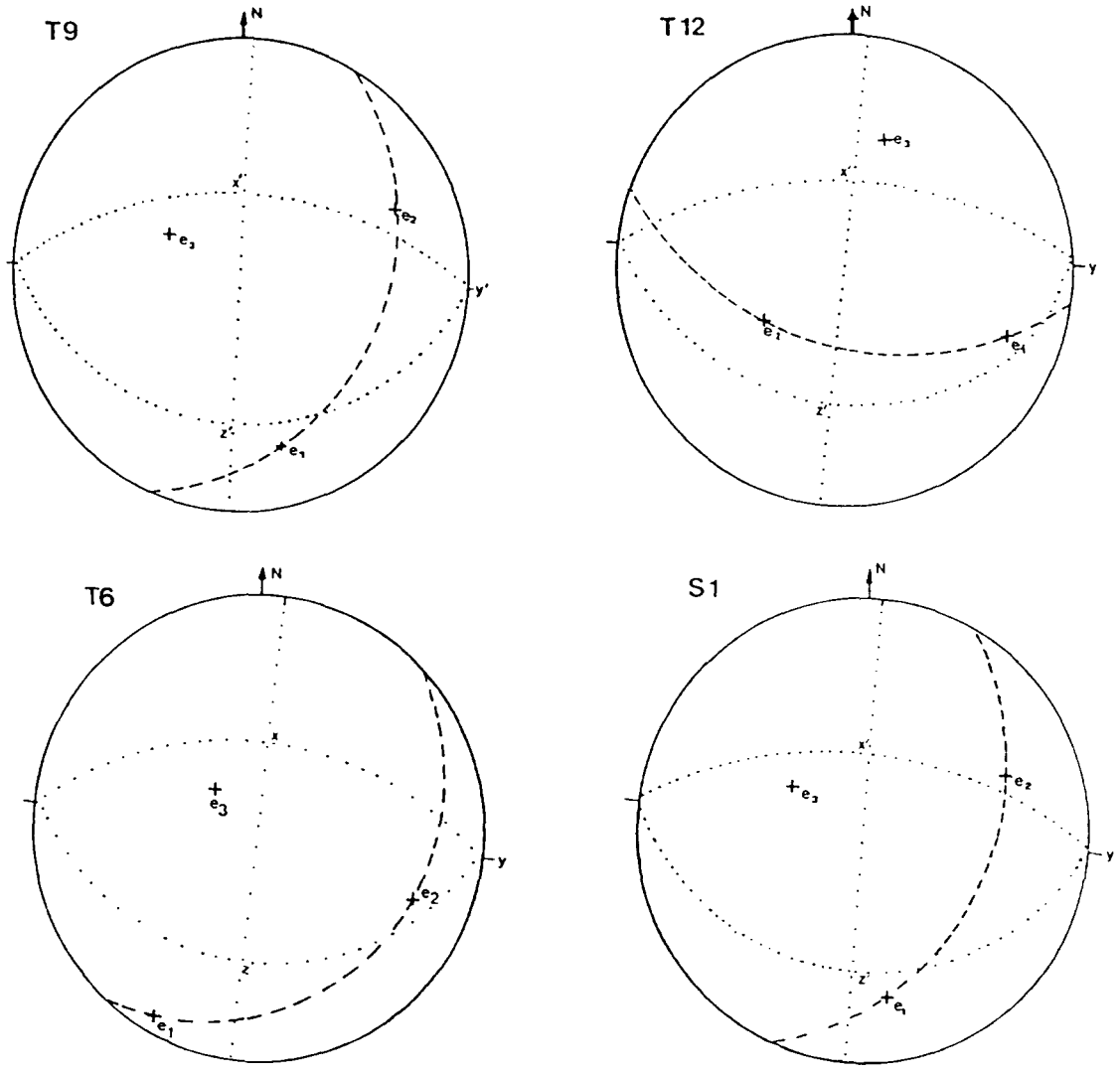

Fig. 14. Stereograms (lower-hemisphere projections) of the three-dimensional strain data for the locations indicated in Fig. 6. The dotted lines refer to the local three-dimensional co-ordinate system ($x'y'z'$) for each specimen, and are the three orthogonal thin sections analysed for each specimen. They are approximately co-axial with the xyz co-ordinate axes. e_1, e_2 and e_3 indicate the principal extension directions.

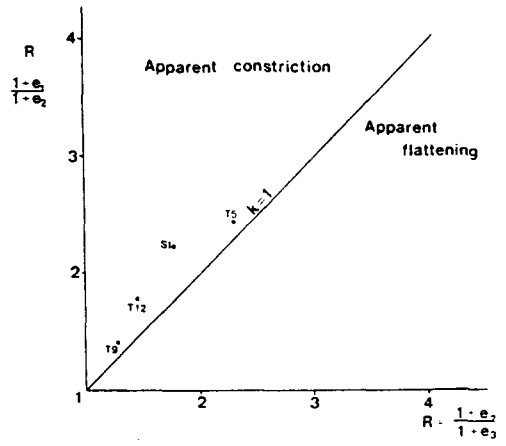

Fig. 15. Flinn plot for the three-dimensional data. The specimen numbers are indicated.

disproportionate straining of the less competent markers.

Two-dimensional strain data from sections cut subparallel to the movement direction are presented in Fig. 6 (x–z plane). The three-dimensional strain data are presented in stereographic form (Fig. 14). A Flinn plot for the three-dimensional data (Fig. 15) indicates that the strain ellipsoids lie in the apparent constriction field. Further details of the strain data are presented by Hyett (1985).

STRESS ANALYSIS

Limited work has been undertaken to determine the palaeostress distribution around the tip of the THTZ, using the Numerical Dynamic Analysis (NDA) technique. This is an alternative method of dynamic analysis proposed by Spang (1972), to determine palaeostresses from calcite twinning. The technique is suitable because it has been well documented (Spang 1972, Spang & van der Lee 1975), has been successfully applied to similar structures (Brown & Spang 1978, Spang & Brown 1981), and can be easily computerized. The technique is a numerical method which avoids the time consuming process of plotting and then contouring the compression and tension axes calculated from each grain. Instead, the eigenvectors of the bulk stress tensor (an average of the incremental strain tensor calculated for each grain, and transformed to a common set of reference axes) are determined numerically (see Spang 1972). The associated eigenvalues depend on the concentration of data points around the eigenvectors, and are high for a population tightly clustered around the eigenvector. The fundamental assumptions of the technique have been verified by Spiers (1981), who reported that for deformation in the twinning field the state of stress can be considered to be relatively homogeneous from grain to grain.

The principal axes of stress obtained from NDA are presented in Fig. 16, on a simplified x–z plane cross-section. In cases where axial or small circle c-axis concentrations existed the technique breaks down. However, despite the problems involved with the interpretation of these data, the author has tentatively inferred that the compression direction is parallel to the c-axis maximum (in the case of axial symmetry), or symmetrically bisects a small circle girdle.

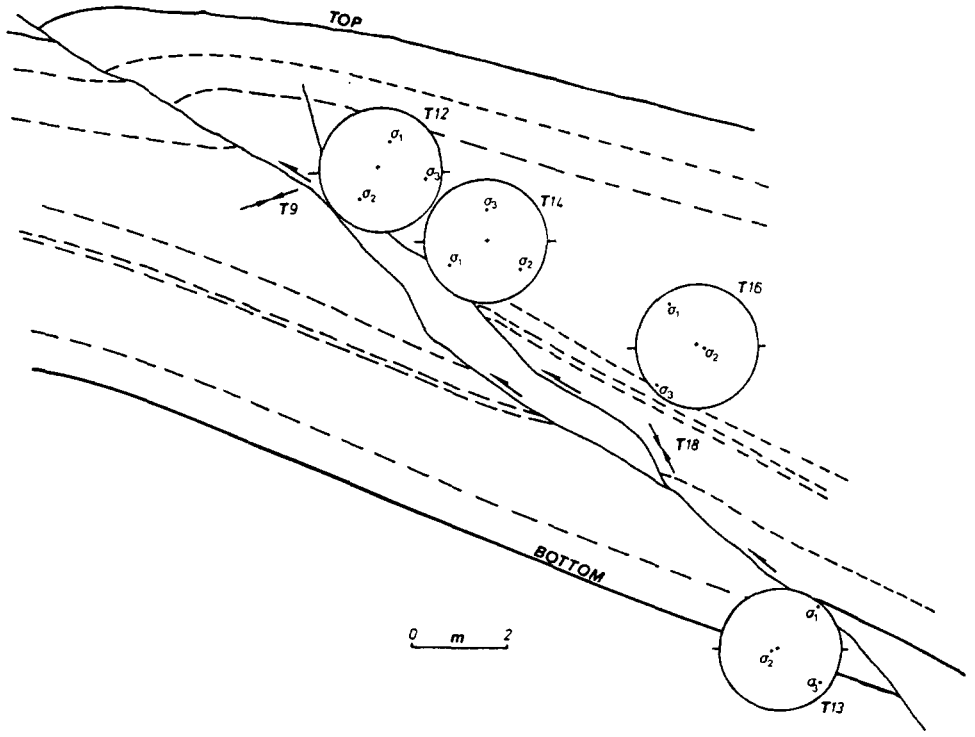

Fig. 16. Simplified cross-section of the tip zone showing stress results. Stereograms show the calculated stress axes using NDA technique. The primitive of each stereogram is the x–z plane, 015°/vertical, and projections are far hemisphere (i.e. east hemisphere). Arrows indicate compression directions inferred from c-axis fabric maxima (see text). The cross at the centre of each stereogram represents the location of the sample.

DISCUSSION

Eshelby (1973) suggested that a fault plane which has undergone limited slip can be treated as a Somigliana dislocation. There are also similarities between the kinematics of a creep event on a fault plane and the movement of a dislocation loop through a crystal plane during intracrystalline slip. The rupture surface on a fault plane is analogous to the slipped region of the crystal lattice. The net slip on the fault is controlled by the magnitude of the creep event and may be thought of as equivalent to the Burgers vector of a dislocation. In both cases if the slip direction is known, the screw, edge or mixed nature of the dislocation can be determined. An edge dislocation, which is analogous to a thrust tip with a propagation direction perpendicular to the tip-line, is often represented by 'an extra half plane' in the crystal lattice. The mechanical characteristics of an edge dislocation, lattice distortion, stress concentration and associated elastic strain energy should have corresponding analogues at a fault tip.

Considerable attention has recently been concentrated on the nature and extent of deformation occurring within ductile beads at the propagating tips of faults. Cooper *et al.* (1982) have shown that in the Henaux Basse Normandy duplex, a zone of ductile layer-parallel shortening advanced in front of the floor thrust. Williams & Chapman (1983) presented a two-dimensional model to illustrate the interrelation between fault plane slip, fault-tip propagation and internal strain. They introduced the distance–displacement plot, and used it to quantify the relative stretch between the hangingwall and the footwall. They applied the technique to a number of natural examples of fold thrust structures. Complimentary experimental work by Rodgers & Rizer (1981) using clay models indicated the shape and extent of concentrated deformation at a fault tip.

In the remainder of this paper the data presented above will be interpreted, and the implications for the mechanics of thrust-tip propagation highlighted. The data enable a field-based evaluation of the existing fault-tip models, and the proposal of some new ones.

Sequential development of the tip zone

Comparison of the restored section with the original mapped section, enables an assessment of the sequential development of the thrust zone. Initial deformation involves intense cataclasis at the base of the coarse grainstone unit and within an extended cataclastic ribbon, which is now preserved within the hangingwall of the tip zone. It is evident that the cataclastic shear zone began to propagate at a steep initial inclination on entering the coarse grainstone unit, possibly in response to stress refraction at the base of the more competent coarse grainstone unit. As propagation advanced and the displacement across the shear zone increased, it became mechanically favourable to short-cut this high-inclination irregularity in the shear zone trace, in order to avoid excessive hangingwall strain. Consequently, a new failure plane propagated through the footwall of the shear zone, and in doing so isolated a relatively undeformed lozenge-shaped wedge of material from near the base of the grainstone unit (Fig. 7). The resultant smoothing of the shear zone trace enabled increased displacement along the shear zone, and the isolated wedge moved forward, behaving like a bulldozer, scraping up and folding the previously generated cataclastic debris in front of it.

Ahead of this zone, a pervasive pressure-solution cleavage developed within the thrust zone, which was subsequently reworked as displacement accumulated. An early pressure-solution cleavage plane provided convenient slip horizons resulting in the imbrication of slivers (in effect 'ductile horses') to form a back steepened imbricate zone, similar in appearance to a foreland thrust imbricate stack. The imbricate zone, which is contained between a roof thrust (RT in Fig. 8) and a floor thrust (FT in Fig. 8), is associated with significant thickening and complimentary displacement reduction. Microscopic observation of samples taken from this zone reveal that early pressure-solution features were progressively overprinted by later plastic microstructures.

Strain data interpretation

The two-dimensional strain data presented in Fig. 6, indicate that the strain increases dramatically towards the centre of the shear zone. Measurements away from the centre (T11, T12 and T9) indicate extension parallel to the fault plane in the footwall and contraction parallel to the fault in the hangingwall. The differences between these values ($e_x^{T9} - e_x^{T11}$ and $e_x^{T9} - e_x^{T12}$) give a rough estimate of the relative stretch (ε_r). These values were compared with estimates of relative stretch obtained from a distance–displacement plot which was constrained using the brachiopod-rich marker horizons (L_1–L_4 in Fig. 6). The agreement, illustrated in Fig. 17, is reasonably good.

The distance–displacement plot also indicates that the displacement reduction is concentrated towards the top of the coarse grainstone unit (above L_3), i.e. that region of the tip zone where crystal plastic deformation was concentrated. Two interpretations for this seem feasible.

(i) The coarse grainstone unit represented an obstacle to fracture propagation and the increased stress concentration required for propagation was sufficient to induce localized plastic deformation and formation of a ductile bead.

(ii) A high level of elastic strain energy existed at the propagating thrust tip, which was relieved by time-dependent relaxation at relatively low strain rates, after the structure became inactive. The inference of extremely low strain rates may explain the observation of microstructures related to dislocation climb mechanisms which usually occur at much higher temperatures (see Shaw 1982, for estimates of thermal history).

The three-dimensional data in Fig. 10, indicates that

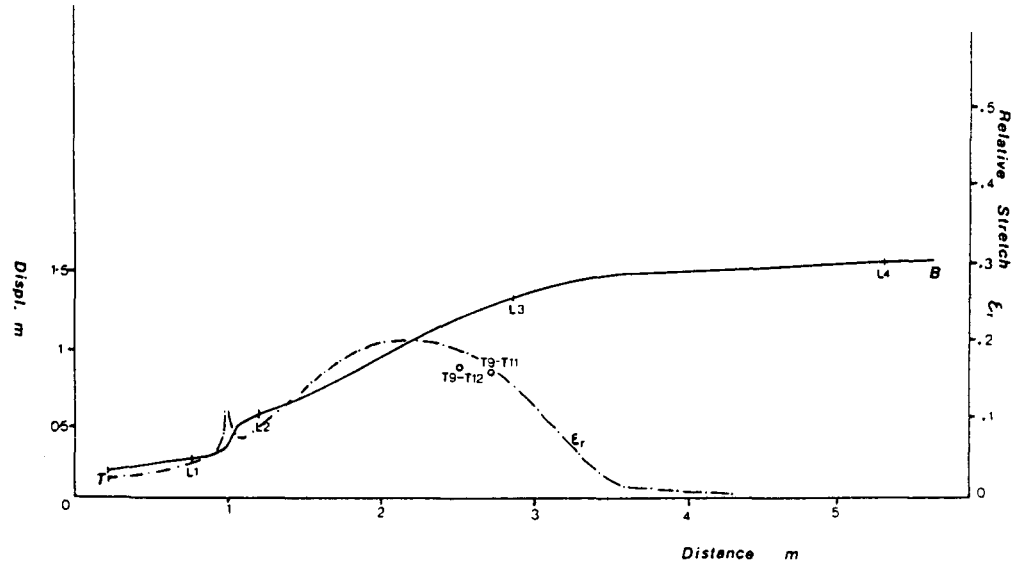

Fig. 17. Distance–displacement graph with corresponding relative stretch graph. The relative stretch values, calculated as described in the text using T9 in association with T11 and T12 are included for comparison. L_1–L_4 correspond to brachiopod-rich marker horizons.

the maximum principal extension (e_1) direction for S1 and T9 is oblique to the movement direction by approximately 30°. The direction of stretching given by these ellipsoids indicates a component of simple shear co-planar with the thrust plane, probably caused by lateral variation in displacement along the tip-line. Two mechanical alternatives, implying different geometrical settings are capable of generating such oblique strains.

(i) *A genuine oblique tip setting*. Oblique tips comprise the majority of the tip-line loop which surrounds an isolated thrust plane. As an oblique tip (analogous to a mixed dislocation) propagates, unless propagation is effortless, a component of shear deformation is induced at the thrust tip (Fig. 18).

(ii) *Tip-line pinning*. Continuing with the dislocation–fault-tip analogy, an equally valid explanation can be developed, which relates to the pinning effect that both a dislocation and a fault tip-line suffer on interaction with an obstacle. If a dislocation becomes pinned, an unpinned portion of it may move forward, initiating bulging, until it is restrained by the pinning effect. As this occurs its driving force will be transferred to the obstacle, which will become the focal point of stress concentration. Stresses will continue to increase until the resistance offered by the obstacle is exceeded.

Consider how this may occur for the tip of the THTZ. The obstacle is the thick grainstone unit at the top of the Seminula Mudstone. The occurrence of a pinning point during propagation is a geometrical necessity because the tip-line inclination is different from the component of bedding plane dip along the tip-line trend (Fig. 19). Hence, if propagation of the thrust tip advances in the thrust plane and in the direction of transport, the tip-line to the west of the exposed tip will have emerged from the obstacle, while that to the east is still within or below it. On emergence from the obstacle propagation is possible at a faster rate. If considerable differential displacement occurs, then a component of shear strain co-planar with the thrust plane or even out-of-section movement will result (Fig. 20).

This shear strain will be concentrated around the pinning point, and its magnitude will depend on such factors as, the strength of the obstacle and the amount of differential movement on either side of the obstacle. Following propagation through the obstacle, the strain

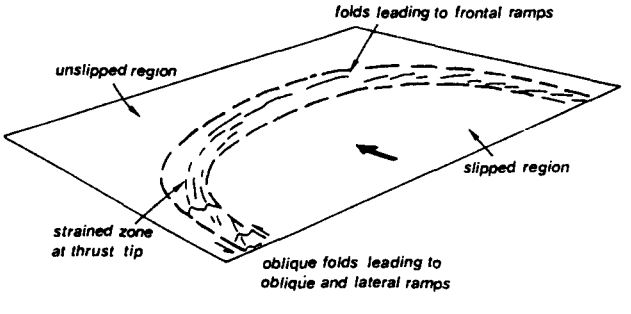

Fig. 18. Strain patterns at the tip of a thrust (Coward & Potts 1983).

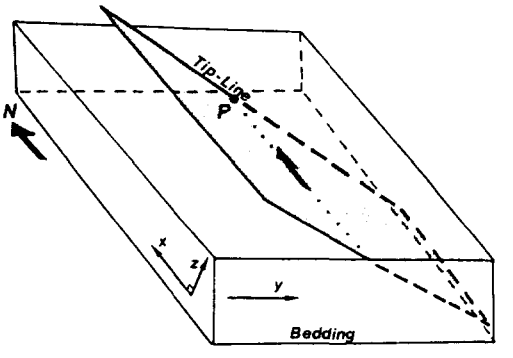

Fig. 19. Orientation of tip-line and bedding. Solid tip-line is above the obstacle, broken is within or below it. P is the location of a pinning point. The dotted line represents the trend of bedding plane cut-offs.

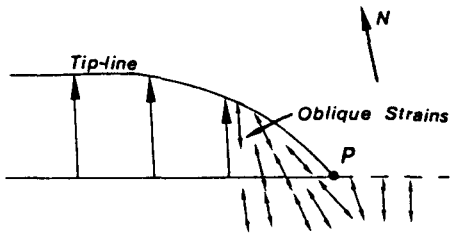

Fig. 20. Schematic diagram indicating the oblique strains developed by tip-line pinning. The diagram represents an exaggerated plan view of Fig. 12. The solid tip-line has emerged from the obstacle and is therefore able to propagate at a faster rate which results in bulging of the tip-line. The double headed arrows refer to the axes of maximum extension.

patterns revert to movement-parallel, as recorded by specimen T5 near the top of the grainstone unit, progressively overprinting the oblique strains. It is quite likely that a contribution from each mechanism operates. However, there is very little evidence to indicate a genuine oblique tip setting (e.g. other oblique or strike-slip structures).

Palaeostress interpretation

The results are not of sufficient density to construct stress trajectories around the thrust tip although several quantitative statements can be made.

Specimens T18 and T16 indicate that, for samples collected far from the thrust tip, principal stresses are orientated with σ_1 parallel to movement in the hangingwall and perpendicular to movement in the footwall. This pattern is basically compatible with the stress distribution around the analogous Type II shear crack (Fig. 21b) (cf. Lawn & Wilshaw 1975). There is evidence that σ_1 becomes considerably inclined to the thrust zone at T9 suggesting development of the cross-over of stress trajectories that occurs in front of the tip. It therefore appears that the stress distribution reflects the tip-zone geometry rather than bedding inclination or stresses due to flexure of the Langland–Mumbles Anticline. This implies that the stress magnitudes resulting from tip zone propagation are in excess of those related to larger scale deformation. Fracture mechanics theory also predicts the distribution of stress magnitudes around a crack tip. Using these in conjunction with Von Mises' yield criteria, McClintock & Irwin (1965) predicted the shape of the plastic zone for a variety of crack geometries, for both plane stress and plane strain conditions; that for Mode II geometry is shown in Fig. 21(c). It should be stated that the analysis does not account for the stress redistribution that will inevitably accompany yielding.

The simple stress pattern outlined above is complicated by a stress perturbation above the zone of imbrication, recorded by specimens T14 and T15. The most obvious development in this region is the reduction in relative magnitude of the stress sub-parallel to the movement direction (at T16 σ_1 is approximately sub-parallel to the movement direction, at T14 σ_2 is parallel, and at T12 σ_3). The occurrence of a measurable stress irregularity above a zone of imbrication and the observed

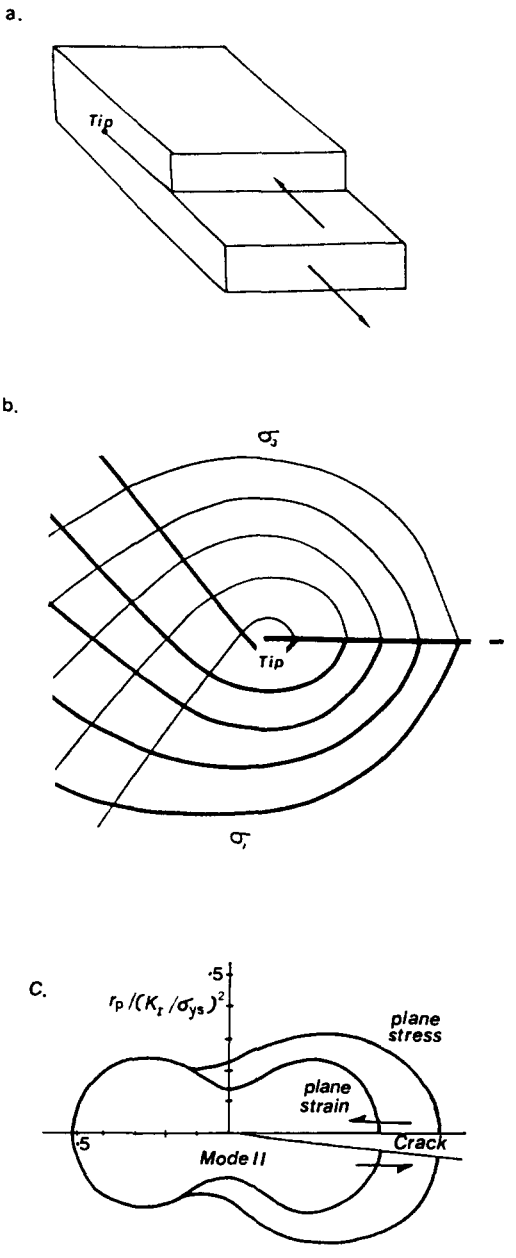

Fig. 21. (a) Geometry of Mode II shear crack. (b) Stress directions around a Mode II shear crack. (c) Plastic zone for a Mode II crack for plane stress and plane strain cases. r_p is the distance away from the crack tip, K_I the Mode I stress intensity factor and σ_{ys} the yield stress.

displacement reduction suggests that thickening within the shear zone, with associated lateral expulsion of material in this region, may cause a localized relative increase in the lateral and vertical stress components. If the calcite twinning is easily reset, then the last increment of deformation will be recorded and this suggests, following the explanation above, that lateral expulsion is more important near the active front of the imbricate zone, than farther back where progressive backsteepening has rendered the zone inactive.

CONCLUSIONS

A detailed field and microscopic investigation has enabled an assessment of both the geometry and mech-

anics of thrust-tip propagation. An interpretation of the deformation mechanisms, the three-dimensional strain pattern and the palaeostress distribution, indicate that the tip of the THTZ is indeed a *ductile bead* of intense, plastic deformation. A transition from early pressure solution accommodated cataclastic deformation to crystal plastic dominated processes remains enigmatic, although the effect of fluid pressure, and strain rate must undoubtedly be important.

Strain and palaeostress determinations indicate locally high strain, and a significant stress concentration accompanies thrust-tip propagation. The observed displacement reduction is predominantly accommodated by fault parallel extension in the footwall, with a relatively minor contribution from fault-parallel hangingwall contraction. The palaeostresses indicate a similar general pattern with σ_3 parallel to the movement direction in the footwall and σ_1 in the hangingwall.

Local variations within the thrust tip were also recorded. The directions of the maximum principal extension at T9 and S1, which are approximately 30° oblique to movement, can be most adequately explained by the orientation of the tip-line with respect to the coarse grainstone unit, which represents an obstacle to propagation. By analogy with the pinning of dislocations, this mechanism has been termed *tip-line pinning*.

Although the discussion of thrust-tip propagation presented in this paper relates to data collected from a specific thrust tip, it is unlikely that the mechanisms are unique to the THTZ. It is probable that similar processes operated at other tip zones, possibly on a much larger scale, although in the majority of cases, the structural information necessary to confirm this does not exist. Furthermore, it is conceivable that structures related to thrust tip deformation should be preserved adjacent to thrust planes, if the evidence has not been overprinted by subsequent displacement related deformation.

Acknowledgements—This paper is a testimony to the quality of teaching on the M.Sc. in Structural Geology and Rock Mechanics at Imperial College. Mike Coward encouraged the author to write this paper and corrected an early version. Considerable improvements also resulted from the attention of the referees; T. J. Chapman, Dave Morley and Dave Sanderson. Finally, thanks to my parents for providing support during the work.

REFERENCES

Bowler, S. 1987. Duplex geometry: an example from the Moine thrust belt. *Tectonophysics* **133**, 25–35.

Brown, S. P. & Spang, J. H. 1978. Geometry and mechanical relation to folds to thrust fault propagation, using a minor thrust in the Front Ranges of the Canadian Rocky Mountains. *Bull. Can. Petrol. Geol.* **26**, 551–571.

Cooper, M. A., Gratton, M. R. & Hossack, J. R. 1982. Strain variation in the Henaux Basse Normandie duplex, northern France. *Tectonophysics* **88**, 321–324.

Coward, M. P. & Potts, G. J. 1983. Complex strain patterns developed at the frontal and lateral tips to shear zones and thrust zones. *J. Struct. Geol.* **5**, 19–32.

Eshelby, J. D. 1973. Dislocation theory for geophysical applications. *Phil. Trans. R. Soc. Lond.* **A274**, 331–338.

Elliot, D. 1976. The energy balance and deformation mechanics of thrust sheets. *Proc. R. Soc. Lond.* **A283**, 289–312.

Fry, N. 1979. Density distribution technique and strained length methods for the determination of finite strains. *J. Struct. Geol.* **1**, 221–229.

Hyett, A. J. 1985. Deformation around a thrust tip in Carboniferous limestone at Tutt Head, near Swansea. Unpublished M.Sc. thesis, University of London.

Lawn, B. R. & Wilshaw, T. R. 1975. *Fracture of Brittle Solids*. Cambridge University Press, London.

McClintock, F. A. & Irwin, G. R. 1965. Plasticity aspects of fracture mechanics. *ASTM* **STP 381**, 84–113.

Shaw, N. D. 1982. Unpublished Ph.D. thesis, University of London.

Spang, J. H. 1972. Numerical method for the dynamic analysis of calcite twin lamellae. *Bull. geol. Soc. Am.* **83**, 467–472.

Spang, J. H. & Brown, S. P. 1981. Dynamic analysis of a small imbricate thrust. In: *Thrust and Nappe Tectonics* (edited by McClay, K. R. & Price, N. J.). *Spec. Publs geol. Soc. Lond.* **9**, 143–149.

Spang, J. H. & van der Lee, J. A. 1975. Numerical dynamic analysis of quartz deformation lamellae and calcite and dolomite twin lamellae. *Bull. geol. Soc. Am.* **86**, 1266–1272.

Spiers, C. J. 1981. The development of deformation textures in calcite rocks. Unpublished Ph.D. thesis, University of London.

Williams, G. D. & Chapman, T. J. 1983. Strains developed in the hanging-walls of thrusts due to their slip/propagation rate; a dislocation model. *J. Struct. Geol.* **5**, 563–571.